The Journal *of* Immunology

A Deficiency in Nucleoside Salvage Impairs Murine Lymphocyte Development, Homeostasis, and Survival

Onjee Choi, Dean A. Heathcote, Ka-Kei Ho, Phillip J. Müller, Hazim Ghani, Eric W.-F. Lam, Philip G. Ashton-Rickardt and Sophie Rutschmann

Supplementary Material	http://www.jimmunol.org/content/suppl/2012/03/13/jimmunol.1102587.DC1.html
References	This article **cites 45 articles**, 19 of which you can access for free at: http://www.jimmunol.org/content/188/8/3920.full#ref-list-1
Subscriptions	Information about subscribing to *The Journal of Immunology* is online at: http://jimmunol.org/subscriptions
Permissions	Submit copyright permission requests at: http://www.aai.org/ji/copyright.html
Email Alerts	Receive free email-alerts when new articles cite this article. Sign up at: http://jimmunol.org/cgi/alerts/etoc

A Deficiency in Nucleoside Salvage Impairs Murine Lymphocyte Development, Homeostasis, and Survival

Onjee Choi,* Dean A. Heathcote,*,[1] Ka-Kei Ho,[†],[1] Phillip J. Müller,* Hazim Ghani,* Eric W.-F. Lam,[†] Philip G. Ashton-Rickardt,* and Sophie Rutschmann*

The homeostasis of the immune system is tightly controlled by both cell-extrinsic and -intrinsic mechanisms. These regulators, not all known to date, drive cells in and out of quiescence when and where required to allow the immune system to function. In this article, we describe a deficiency in deoxycytidine kinase (DCK), one of the major enzymes of the nucleoside salvage pathway, which affects peripheral T cell homeostatic proliferation and survival. As a result of an *N*-ethyl-*N*-nitrosourea–induced mutation in the last α helix of DCK, a functionally null protein has been generated in the mouse and affects the composition of the hematopoietic system. Both B and T lymphocyte development is impaired, leading to a state of chronic lymphopenia and to a significant increase in the number of myeloid cells and erythrocytes. In the periphery, we found that mutant lymphocytes adopt a CD44^{high}CD62L^{low} memory phenotype, with high levels of proliferation and apoptosis. These phenotypes are notably the result of a cell-extrinsic–driven lymphopenia-induced proliferation as wild-type cells transferred into DCK-deficient recipients adopt the same profile. In addition, DCK also regulates lymphocyte quiescence in a cell-intrinsic manner. These data establish *dCK* as a new regulator of hematopoietic integrity and lymphocyte quiescence and survival.   *The Journal of Immunology*, 2012, 188: 3920–3927.

T hroughout development and adult life, the immune system relies on homeostatic mechanisms to adjust to the many challenges it faces to maintain itself but also to respond to self- and pathogenic Ags. In healthy unchallenged individuals, the rate of peripheral homeostatic proliferation remains low and hematopoietic cells are quiescent, conserving metabolic resources to survive for long periods, but also preventing from accumulating malignant metabolic and/or genetic damages (1). This quiescence of hematopoietic cells is actively positively and negatively maintained by both cell-intrinsic and -extrinsic factors, such as Forkhead box transcription factors, Tob, and cytokines (IL-2, -7, and -15) (1–5). Genetic deficiencies in these regulators can result in severe human syndromes, ranging from acute and chronic leukemia to several myeloproliferative diseases (3, 5, 6). However, not all the mechanisms that control hematopoietic homeostasis are known to date, and large numbers of patients are likely to harbor

different genetic defects (6). In the course of an immune response, the activation of resting naive T cells by APCs will drive them out of their quiescent state to undergo a massive phase of cellular proliferation (7). Once the Ag is cleared from the host, most of these T cells will die to maintain the homeostasis of the T cell pool. Few Ag-specific T cells will survive and re-enter quiescence to prevent replicative senescence. These memory cells will remain in the host for long periods of time and provide a rapid and efficient protection to secondary infections. These events have been well described in the context of CD8$^+$ T cell immune response to viral infections, which therefore provides a good model to identify new regulators of hematopoietic homeostasis.

In the cell, purine and pyrimidine nucleotides are synthesized by both de novo and salvage pathways that generate nucleotides from ribonucleoside diphosphate and deoxynucleoside, respectively (8). The salvage pathway is notably composed of four enzymes with overlapping specificities for the four native DNA precursors. These control the rate-limiting phosphorylation of deoxynucleoside step: dCK and thymidine kinase 1 (TK1) in the cytosol, and mitochondrial thymidine kinase 2 (TK2) and deoxyguanosine kinase (9). In particular, DCK directly phosphorylates deoxyadenosine, deoxycytidine, and deoxyguanosine. Additional enzymes are also involved, for example, hypoxanthine phosphoribosyl transferase or adenosine deaminase (ADA). Deficiencies in purine and pyrimidine salvage have been associated with several human syndromes with many different symptoms (10). These include the neurologic disease Lesch–Nyhan syndrome, caused by hypoxanthine phosphoribosyl transferase deficiency, and the immunological defect SCID, caused by deficiency of either ADA or purine nucleoside phosphorylase (11–13). Deficiencies in deoxyguanosine kinase and TK2 result in mitochondrial DNA depletion with fatal outcomes in both humans and mice (14–16). Mice deficient for TK1 develop kidney disease, whereas those deficient for dCK display altered lymphocyte development (17, 18). In humans, a reduction in DCK enzymatic activity has been associated with resistance to antiviral and anticancer chemotherapeutic agents, whereas increased DCK enzymatic activity is associated with increased ac-

tivation of these compounds to cytotoxic nucleoside triphosphate derivatives (19–21).

In this study, we report a null murine dCK mutant strain, memory IL-7R phenotype (*memi*), which presents, in addition to lymphocyte developmental deficiencies, changes in peripheral hematopoietic populations and a very high rate of cellular proliferation associated with an increased level of cell death in peripheral lymphocytes. Our data indicate that this increased proliferation is due to both cell-extrinsic and -intrinsic effects. Our mouse model therefore supports an unexpected nonredundant role for dCK in homeostasis and survival of immune cells.

Materials and Methods

Mice, mutagenesis, and lymphocytic choriomeningitis virus infection

The *memi* mutant mice were generated in a C57BL/6J background (C57BL/6J, Thy1.1, and 129SvlmJ purchased from Charles River, Lille, France) and bred in Central Biomedical Services (Imperial College London, London, U.K.). Mice were kept under specific pathogen-free conditions in individually ventilated cages. All animal procedures have been authorized in a British Home Office Animals Act License (PPL:70/6490). The *N*-ethyl-*N*-nitrosourea (ENU) mutagenesis was performed as previously described (22). For the infection, mice were injected i.p. with 2×10^5 PFU lymphocytic choriomeningitis virus (LCMV) Armstrong. At days 8 and 21 after the injection, lateral vein blood was analyzed by flow cytometry.

Cell preparation and flow cytometry

Spleen and blood cells were incubated 5 min at room temperature in an RBC lysis buffer (0.85% [w/v] NH_4Cl, 50 mM Tris, pH 7.2). All Abs were from eBioscience (Hatfield, U.K.) except CD8 and TCRVβ8 (BD Bioscience, Oxford, U.K.). LCMV-specific cells were detected with a PE-conjugated gp33-iTAg MHC class I tetramer (Beckman Coulter). The analysis of apoptosis was performed with an Annexin V/PI kit (BD Bioscience). For proliferation and cell cycle, a Ki67 or an anti-BrdU Ab/7-aminoactinomycin D kit was used (BD Bioscience). For BrdU experiments, mice were given freshly prepared 0.8 mg/ml BrdU (Sigma, Dorset, U.K.) in drinking water daily for 5 d. Samples were acquired on a DAKO Cyan 9 flow cytometer, and data were analyzed with Summit software.

dCK sequencing

The 7dCK exons were amplified from genomic DNA by PCR using the JumpStart REDTaq ReadyMix (Sigma). PCR samples were purified by Qiagen PCR purification kit (Qiagen, Crawley, U.K.), sequenced (Genomic Laboratory, Imperial College, London, U.K.), and the data analyzed with the Sequencher software (Gene Codes Corporation). The settings were: initialization 2 min/94˚C, denaturation 30 s/94˚C, annealing 30 s/60˚C, extension 90 s/72˚C.

Primers were as follows: exon 1 (CGAGATTGACGCTGCAACC/AAGGGTGCACACTGGTCCAG), exon 2 (GATGATGGTTGGTTATAGTTTGC/GCAGCTGTAGCTGGTTAGGAG), exon 3 (AGCAACGTAGTGAGACCTTATC/CGCAGCCTCTAATTTGATTACC), exon 4 (TGTTTGAAAGGATGTCCATGC/TTTCAACAACACAGGCAAATG), exon 5 (ACGGCAGCAGACACAACTAG/ACAGTGAGCAGCAACCAGC), exon 6 (GCATCACTACGGATGACGTTAG/TGTCCTGGACAAGACAAGACAC), and exon 7 (GGTTATTCAACCTACTACTGAAATACTTAG/CCACTCACTGCCCTGATGC).

CD4+ T cell transfer and bone marrow chimera

Splenic CD4+ T cells from *Thy1.2;dCK^mem/mem^* or Thy1.1;dCK^+/+^ congenic mice were purified with magnetic beads (Miltenyi Biotec, Church Lane Bisley, U.K.). Three to 5 million cells from those donor groups were injected i.v. to nonirradiated *Thy1.2;dCK^mem/mem^* or Thy1.1;dCK^+/+^ recipients. For bone marrow (BM) chimera, Thy1.1;dCK^+/+^ wild-type (wt) recipients were fed antibiotics in the drinking water for 2 d and subsequently lethally irradiated with 900 rad. BM cells from either Thy1.1;dCK^+/+^ wt or *Thy1.2;dCK^mem/mem^* mice were obtained, and mature T cells were removed with *Pan*-T cell magnetic beads (Miltenyi Biotec). The BM cells were then mixed at a 1:1 ratio, and 10^6 were injected i.v. into each recipient mouse. These were analyzed 5 wk after injection.

dCK kinase activity assay

Proteins were extracted by M-PER Mammalian Protein Extraction Reagent (Pierce, Cramlington, U.K.). Protein lysate (5 μg) was incubated in DCK buffer (50 mM Tris-HCL [pH 7.6]; 5 mM UTP; 5 mM $MgCl_2$; 2 mM DTT; 10 mM NaF; 1 mM thymidine) and the addition of 1 μCi 3H-CdA in final volume of 10 μl. Reactions were carried out at 37˚C for 20 min, quenched with 40 μl ice-cold water, and heated at 90˚C for 2 min. The reactions were aspirated onto a Wallac filter mat (Tomtec harvester 9600; Tomtec; and Wallac 1450-421; PerkinElmer, Cambridge, U.K.), washed three times in PBS, three times in 200 ml of 4 mM ammonium formate, and twice for 2 min in 95% ethanol. The filter mat was placed at 60˚C for 10 min before addition of scintillation fluid. Enzyme kinetic properties were calculated by linear regression analysis using Michaelis–Menten plots.

SDS-PAGE and Western blot

Twenty micrograms of spleen proteins were size fractionized by SDS-PAGE and electrophoretically transferred onto nitrocellulose membrane (GE Healthcare, Little Chalfont, U.K.) (23). The primary Abs used are cyclin A (C-19), cyclin D3 (18B6-10), p27Kip1 (C-19), pRB (C-15; Santa Cruz), actin (Abcam, Cambridge, U.K.), Foxo3a (Millipore), and p32-Foxo3a (Cell Signaling). Secondary Abs were rabbit anti-goat (Southern Biotech), goat anti-rabbit, and goat anti-mouse (Dako, U.K.).

Statistical analysis

All results are given as mean values with SD. Nonparametric unpaired *t* test (two-tailed) was applied: $*p < 0.05$, $**p < 0.01$, $***p < 0.001$. All statistical calculations were performed with the Prism5 software (GraphPad).

Results

The ENU-induced mutation memi impairs the immune response to viral infection

To identify new regulators of immune homeostasis, we have undertaken a germline mutagenesis and used the CD8+ T cell response to LCMV infection as a model to screen individual mutant mice. To this end, we have generated a library of third-generation ENU-induced germline mutants in a pure C57BL/6J background. A total of 1480 individual mice were screened for modifications of immune responsiveness to LCMV. Their CD8+ response was assessed by measuring the percentage of Ag-specific CTL (gp33+ CD8+) and of effectors and memory precursors in the blood at the peak of expansion (day 8 postinfection) and at the end of contraction (day 21). Four independent germline transmissible mutations that modify responsiveness to LCMV were isolated, of which a purely recessive one, *memi*, was bred to homozygosity. After LCMV infection, homozygous *memi* mutants mount an Ag-specific CD8+ T cell response, which is highly variable between individuals (Fig. 1A). The Ag-specific population in *memi* mice is significantly enriched in effector cells (KLRG1+IL-7R− gp33+ CD8+) and deprived of memory precursors (KLRG1−IL-7R+ gp33+CD8+; Fig. 1B) (24). In addition, uninfected (naive) *memi* mutants are characterized by a dramatic decrease in CD4+ and B220+ lymphocytes and a significant increase in cells of myeloid origin in the blood (Fig. 1C). These data indicate that the *memi* mutation affects a gene essential for a qualitatively and quantitatively normal CD8+ T cell immune response to LCMV infection, and for a normal hematopoietic composition in the blood.

memi is a null mutation in dCK

To identify the causative *memi* mutation, we used a meiotic positional cloning strategy (25). Mice carrying the *memi* mutation were crossed to the 129SvlmJ strain to obtain first-generation hybrids, which when intercrossed generated 21 second-generation hybrids. These 42 meiotic events were analyzed for the linkage between 358 single nucleotide polymorphisms and the deficiency in CD4+ and B220+ blood lymphocytes, mapping the *memi* mutation to a 13.8-Mb region on chromosome 5 with a logarithm of odds score of 5 (data not shown). This region
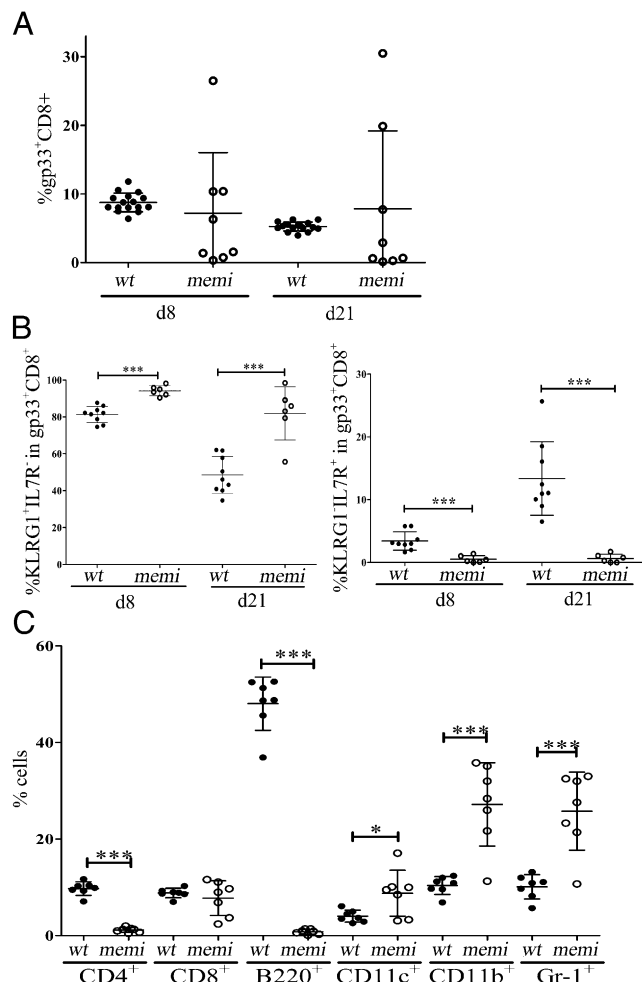
FIGURE 1. *memi* mice present a distinctive immune response upon LCMV infection and a mutant peripheral blood composition in naive conditions. (**A**) Six-wk-old wt and *memi* mice were injected with LCMV Armstrong and their Ag-specific CD8$^+$ T cells (gp33$^+$CD8$^+$) measured at days 8 and 21 after infection. The graph is representative of at least 12 independent experiments. $n = 18$ for wt and 9 for *memi*. (**B**) Wt and *memi* mice were injected with LCMV Armstrong and their effector (KLRG1$^+$IL-7R$^-$gp33$^+$CD8$^+$, *left graph*) and memory precursors (KLRG1$^-$IL-7R$^+$ gp33$^+$CD8$^+$, *right graph*) T cells measured 8 and 21 d postinfection. The graphs are representative of at least 12 independent experiments. $n = 9$ for wt and 6 for *memi*. (**C**) Peripheral blood was stained with specific Abs against lymphocytes and myeloid cells, and analyzed by flow cytometry. These data are representative of five independent experiments. $n = 7$ for wt and *memi*. In all experiments, error bars represent SD; *$p < 0.05$, ***$p < 0.001$.

contains 112 genes and pseudogenes (ensembl version 37.2), notably *dCK* encoding DCK, which was considered a strong candidate based on the T cell phenotype described for the knockout mutant (*dCK*$^{-/-}$) (18). Sequencing of *dCK* at the genomic DNA level in *memi* mice revealed a single nucleotide transversion (G to T) at nucleotide 739 (Fig. 2A). This modification changes the glutamic acid 247 into an early translational terminating codon, removing the last 14 aa of DCK.

To define the nature of the *memi* mutation, we measured DCK-specific enzymatic activity in *dCK*$^{mem/mem}$, *dCK*$^{mem/+}$, and dCK$^{+/+}$ wt mice. As negative and positive controls, we used *dCK*-deficient cells (L1210-10K) and their parental mouse lymphocytic leukemia line L1210, respectively (Fig. 2B) (26). The L1210-10K *dCK*-deficient cell line was generated by growing L1210 leukemic cells
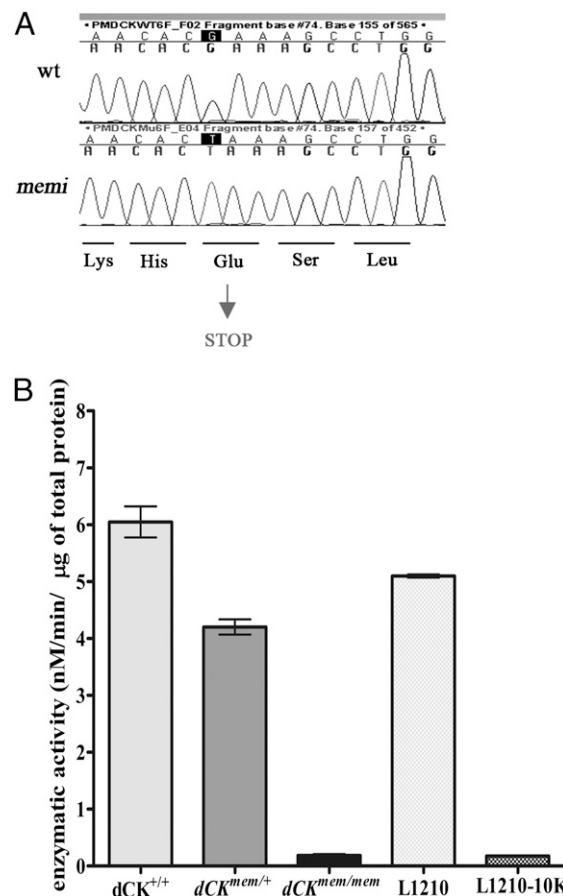
FIGURE 2. *memi* is a null point mutation in *dCK*. (**A**) The *memi* mutation is a single nucleotide transversion (G to T) at nucleotide 739 in exon 6 of *dCK*. This modification changes the glutamic acid (Glu) 247 into an early translational terminating codon (STOP). (**B**) In vitro DCK enzymatic activity assay was performed using cell lysates from *dCK*$^{mem/mem}$, *dCK*$^{mem/+}$, and dCK$^{+/+}$ spleens. L1210 and L1210-10K cell lines were used as positive and negative controls (26). The graph is representative of two independent experiments in which DCK activity was analyzed in triplicate with samples pooled from three mice per genotype.

in the presence of increasing concentration of gemcitabine. We found that the specific DCK enzymatic activity in *dCK*$^{mem/mem}$ splenocytes was reduced to the background levels observed in L1210-10K cells. This reduction in functionality was not due to an effect of the mutation on the mRNA or protein expression because both are produced normally in *dCK*$^{mem/mem}$ cells (Supplemental Fig. 1). These data indicate that our point mutation abolishes DCK functional activity in homozygous mice to levels found in *dCK*-deficient cells, establishing our point mutation *dCK*$^{mem/mem}$ as a new recessive null allele of *dCK*.

B and T lymphocyte development defects in *dCK*$^{mem/mem}$ mice

The analysis of *dCK*$^{-/-}$ mice implicated a role for the kinase in T and B cell development (18). The analysis of B cell development showed a significant increase in the pro-B cell fractions A–C, correlating with a significant decrease in the pre-B cell fraction D (Supplemental Fig. 2).

dCK$^{mem/mem}$ thymuses were found to be reduced in size and cellularity (Fig. 3A). In the thymus, T cell precursors develop via the following chronological stages: double-negative 1 (DN1; CD4$^-$CD8$^-$CD44$^+$CD25$^-$), DN2 (CD44$^+$CD25$^+$), DN3 (CD44$^-$
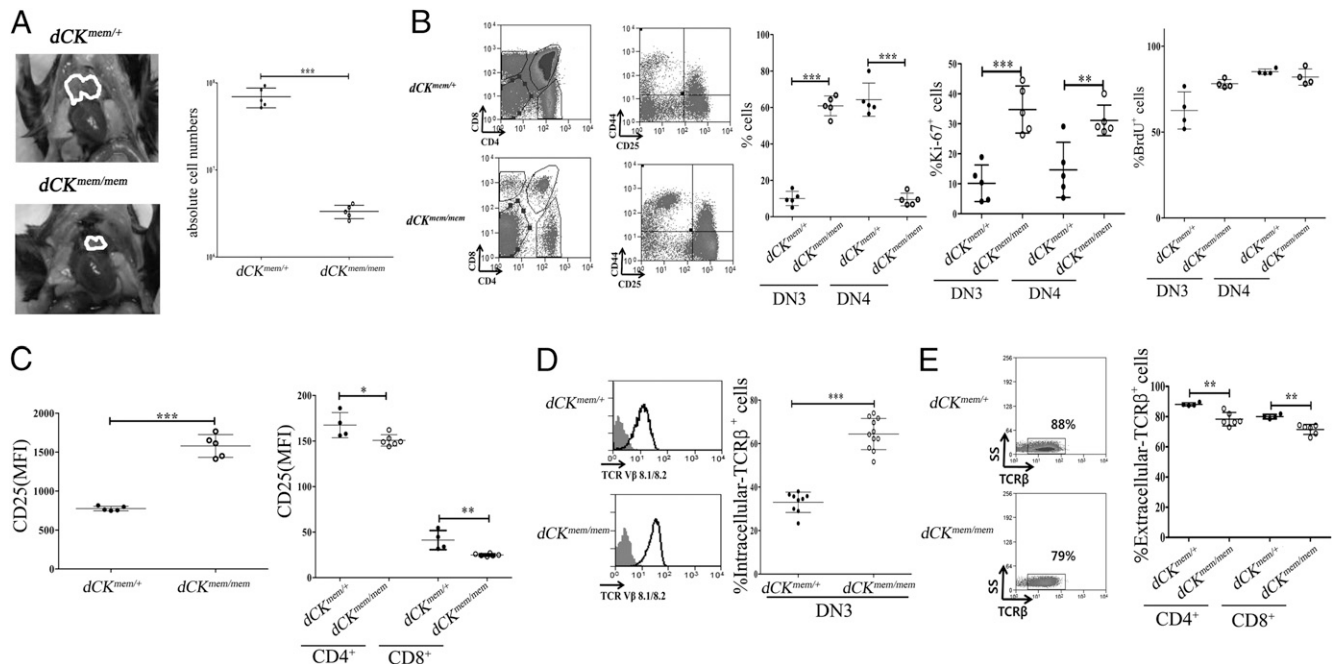
FIGURE 3. *dCK*[mem/mem] mice have profound defects in lymphocyte development. (**A**) *dCK*[mem/mem] mice have reduced thymic size and cellularity. Thymi of two representative mice are indicated by the white lines. The graph is representative of four independent experiments; $n \geq 3$. (**B**) *dCK*[mem/mem] T cells development is blocked at the transition between the DN3 and DN4 stages. The dot plots are from two representative mice, the graph representative of three independent experiments; $n = 5$. Proliferation of mutant DN3 and DN4 cells was assessed by measuring Ki67 expression (*middle graph*) or BrdU incorporation (*right graph*). The graphs are representative of two independent experiments; $n \geq 4$. (**C**) The mean fluorescence intensity (MFI) obtained for CD25 expression in the DN3 population (*left panel*) and in peripheral cells (*right panel*) is indicated. These data are representative of three independent experiments; $n \geq 4$. (**D**) Expression of intracellular TCR-Vβ8.1/8.2 in DN3 thymocytes. The histograms are of two representative mice with TCRβ^- DN1 control (gray) and DN3 cells (black). The graph is representative of two independent experiments; $n \geq 4$. (**E**) Surface expression of TCRβ on peripheral T lymphocytes. The histograms are of two representative mice and the data representative of two independent experiments; $n \geq 4$. In all experiments, error bars represent SD; *$p < 0.05$, **$p < 0.01$, ***$p < 0.001$.

CD25$^+$), DN4 (CD44$^-$CD25$^-$), double positive (CD4$^+$CD8$^+$), and finally, single positive (CD4$^+$ or CD8$^+$). In *dCK*[mem/mem] thymus, we observed a developmental blockage between the DN3 and DN4 stages (Fig. 3B). Proliferation was significantly higher in mutant cells as shown by the increased expression of Ki67, a protein expressed in all cycling/nonquiescent cells. Interestingly, when assessed by BrdU incorporation over a 5-d period, proliferation was found to be increased only in DN3 cells and wt in DN4 cells. Remarkably, the IL-2R α-chain CD25 was expressed at significantly higher levels by the mutant DN3 population (Fig. 3C), a phenomenon observed in mice with defective pre-TCR signaling (27, 28). The expression of CD25 was similar to wt levels on peripheral cells. Finally, we were able to measure wt levels of intracellular TCRβ in mutant DN3 cells (Fig. 3D) and only slightly reduced levels of extracellular TCRβ expression on mutant peripheral lymphocytes (Fig. 3E). Taken together, our data indicate that the *memi* mutation dramatically impairs both pro- to pre-B and DN3 to DN4 T lymphocyte development in a manner similar to the *dCK*$^{-/-}$ knockout model (18). This impairment is, however, incomplete, because some B and T cells are found in the periphery (Fig. 1C).

Splenomegaly and spleen composition in dCK[mem/mem] mice

In the periphery, we found that *dCK*[mem/mem] mice had much enlarged spleens (Fig. 4A), with a significant increase in the absolute number of Ter119$^+$-erythrocyte precursors and of myeloid cells (CD11b$^+$, CD11c$^+$, Gr1$^+$, or Ly-6A$^+$; Fig. 4B). In the lymphocytic populations, CD4$^+$ T and B220$^+$ B cells were consistently decreased in numbers, whereas CD8$^+$ T lymphocytes were present in absolute cell numbers equivalent to wt controls.

Increased proliferation of dCK[mem/mem] peripheral T lymphocytes

Our observation that LCMV-specific CD8$^+$ T cells expressed high levels of KLRG1, a marker associated with replicative senescence (Fig. 1B), prompted us to investigate the proliferative status of *dCK*[mem/mem] peripheral T cells. BrdU incorporation was significantly increased in both mutant T cell subpopulations (Fig. 5A) and confirmed by the increased expression of Ki67 (Supplemental Fig. 3). In vivo, this increase correlated with a significantly greater ratio of cells with an effector memory phenotype, CD44^{high} CD62L^{low} (Fig. 5B), and with an increased level of activation (Supplemental Fig. 3) (29). This memory phenotype in the absence of Ag could imply a role for DCK in homeostatic proliferation.

To further confirm the change in proliferative status, we analyzed splenocytes ex vivo for their cell-cycle progression pattern (Fig. 5C). We observed a significant decrease in the G$_0$/G$_1$ population, correlating with a significant increase in S-phase cells (Supplemental Fig. 4). We investigated cell-cycle regulators in whole-spleen extracts from *dCK*[mem/mem], *dCK*[mem/+], and dCK$^{+/+}$ mice (Fig. 5D). In *dCK*[mem/mem] cells, both cyclin D3 and cyclin A were expressed at higher levels than in wt controls, whereas p27Kip1 and pRb levels were decreased or undetectable. Protein extracts from lymph nodes confirmed those data. Finally, we found that the transcription factor Foxo3a was constitutively inactivated in *dCK*[mem/mem] splenocytes. These data indicate that the decreased quiescence observed in *dCK*[mem/mem] peripheral lymphocytes correlates with changes in the expression of cyclins and their co-regulators.
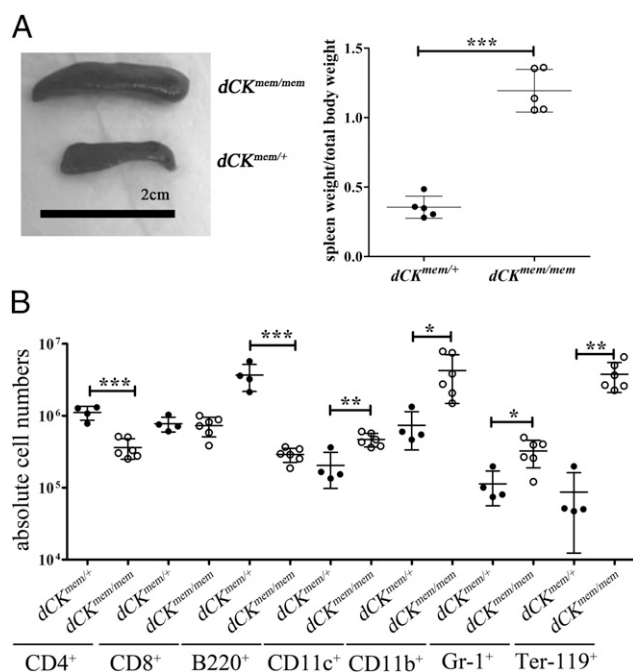
FIGURE 4. *dCK^{mem/mem}* mice present an important splenomegaly because of an increase in nonlymphoid cells. (**A**) Spleens from two representative *dCK^{mem/mem}* and dCK^{mem/+} mice. The relative spleen weights were obtained by dividing individual spleen weights by the corresponding total body weight; $n = 5$. (**B**) Spleen composition in *dCK^{mem/mem}* and dCK^{mem/+} mice. Graph is representative of three independent experiments; $n \geq 3$. Similar data have been obtained for B cells with a CD19-specific Ab.

Increased apoptosis of dCK^{mem/mem} peripheral lymphocytes

The significant increase in proliferation observed in *dCK^{mem/mem}* CD4^+ T cells was not sufficient to restore absolute cell numbers equivalent to those found in wt controls, suggesting that survival might also be affected by the mutation. We therefore measured the population of Annexin V^+/PI^− lymphocytes and found that both CD4^+ and CD8^+ T cells displayed a significant increase in apoptosis (Fig. 5E). This correlated with an increase in the amount of active caspase-3 (Supplemental Fig. 4), confirming that *memi* mutant T cells undergo a greater rate of apoptotic cell death in the periphery.

dCK^{mem/mem} increases proliferation and apoptosis in both a cell-intrinsic and -extrinsic manner

We next asked whether the proliferation, the cell death, or both resulted from a cell-intrinsic or -extrinsic effect of the mutation. To do so, we transferred either Thy1.1;dCK^{+/+}CD4^+ T cells into *Thy1.2;dCK^{mem/mem}* recipients or *Thy1.2;dCK^{mem/mem}* CD4^+ T cells into Thy1.1;dCK^{+/+} recipients (Fig. 6A). At various time points, recipient blood was analyzed for the ratio of donor cells in the CD4^+ compartment. In *memi* hosts 6 d after injection onward, we observed a significant augmentation in Thy1.1;dCK^{+/+} donor cell ratio in the CD4^+ compartment (Fig. 6B), suggesting an increase in wt donor cell proliferation. This increase in proliferation was confirmed when we measured Ki67 expression in splenic donor and endogenous cells 35 d after injection (Fig. 6C). We indeed found that Ki67 expression was significantly higher in Thy1.1;dCK^{+/+} donor cells in *memi* recipients than in Thy1.1; dCK^{+/+} endogenous wt recipients cells.

In wt hosts, *Thy1.2;dCK^{mem/mem}* donor cell ratios remained very low (Fig. 6B), indicating that either *memi* cells have reverted to a quiescent naive phenotype or their level of proliferation is compensated by a high level of cell death. Interestingly, the analysis of

Ki67 expression in the splenocytes of wt recipients (Fig. 6C) indicated that the level of proliferation in *Thy1.2;dCK^{mem/mem}* donor cells was equivalent to the *Thy1.2;dCK^{mem/mem}* endogenous cells in *memi* recipients and significantly higher than the Thy1.1;dCK^{+/+} endogenous cells of the wt host. These data would indicate that even 35 d after transfer into a wt environment, the DCK-deficient *memi* cells are still highly proliferative. We therefore analyzed cell death in the spleen of recipient mice 35 d after injection (Fig. 6D). We found that the level of apoptosis in Thy1.1;dCK^{+/+} donor cells in *memi* recipient was significantly greater than in both *Thy1.2; dCK^{mem/mem}* and Thy1.1;dCK^{+/+} endogenous cells. As expected, the rate of apoptosis in *Thy1.2;dCK^{mem/mem}* donor cells in wt recipients was high and equivalent to the one in *Thy1.2;dCK^{mem/mem}* endogenous cells in the *memi* recipients.
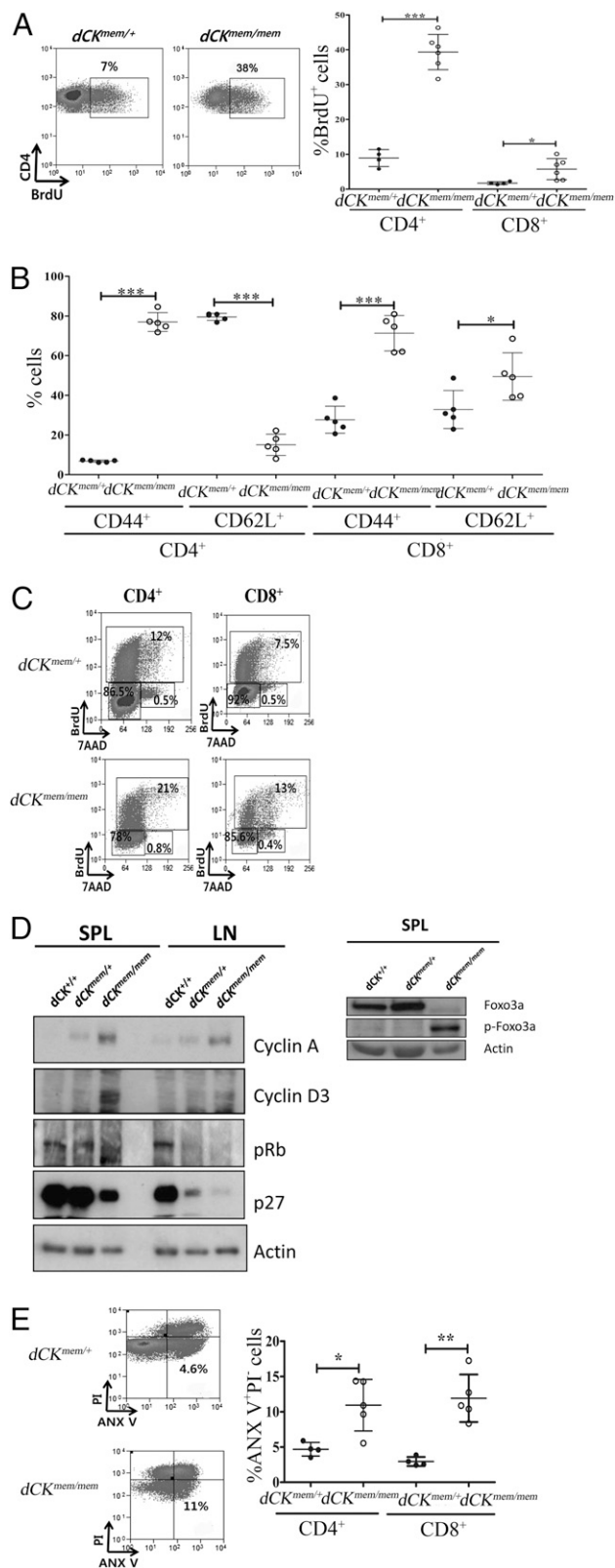
The increased proliferation and maturation of wt CD4^+ T cells in the *memi* host strongly supports a model of homeostatic proliferation in response to the lymphopenic DCK-deficient environment. This is accompanied by a high rate of apoptosis, as has been previously described for cells undergoing lymphopenia-induced proliferation (LIP) (30, 31). Interestingly, the data obtained with *Thy1.2;dCK^{mem/mem}* donor cells in wt recipients seemed to indicate that the absence of functional DCK could also control proliferation and cell death in a cell-intrinsic manner. *memi*'s cell-intrinsic effect was further investigated in 1:1 chimera mice. Lethally irradiated wt recipient mice were injected with a 1:1 *Thy1.2;dCK^{mem/mem}*:Thy1.1;dCK^{+/+} mixture of BM cells depleted of their mature T cells. Five weeks after the injection, at least 95% of thymic and splenic cells were derived from wt progenitors, indicating that *memi* cells are outcompeted by wt cells during reconstitution (data not shown). In the thymus, the development of *Thy1.2;dCK^{mem/mem}* thymocytes was impaired at the transition between DN3 and DN4 stages (Fig. 7A). In the periphery, both proliferation and apoptosis were significantly increased in *Thy1.2;dCK^{mem/mem}* cells as compared with coinjected Thy1.1;dCK^{+/+} controls (Fig. 7B). Altogether, these data indicate that *memi* impairs thymocyte development and induces excessive proliferation and apoptosis of peripheral T lymphocytes in a cell-intrinsic manner.

Discussion

Our study describes a new point mutation in *dCK* and shows that it qdoes not only impair lymphocyte development but also reduces quiescence and survival of peripheral hematopoietic cells. Our *dCK^{mem/mem}* null mutation affects lymphocyte development in a manner similar to that reported for deletional deficiency in the *dCK^{−/−}* knockout mouse (18). The phenotypes of both *dCK^{−/−}* and *dCK^{mem/mem}* mice indicate that DCK is dispensable for non-hematopoietic developmental programs, but demonstrate an essential and nonredundant role for the protein in lymphopoiesis. In addition, our point mutation *memi* reveals an unexpected role for the nucleoside salvage pathway in the regulation of T cell homeostatic proliferation and survival.

In the BM, *memi* B cell development is impaired at the transition between pro-B B220^+CD43^+ and pre-B B220^+CD43^− cells. These are the stages at which Ig heavy V(D)J rearrangement takes place. In T cells, V(D)J recombination and TCRβ rearrangement take place at the DN3 stage. Cells with TCRβ that cannot rearrange properly die of apoptosis. The TCRβ-chain covalently couples to the pre-T α-chain and CD3 to form the pre-TCR complex. In the absence of pre-TCR signaling, thymocyte development is severely affected at the DN3 to DN4 transition.

In their article, Toy et al. propose two major hypotheses that could account for the T lymphocyte development defects observed in *dCK^{−/−}* mice (18). The first one would be that a deficiency in

DCK and deoxynucleotide salvage impairs the considerable proliferation occurring at the DN3 stage, therefore reducing the DN4 population. However, in our hands with Ki67 expression, proliferation is significantly higher in mutant thymocytes (Fig. 3B). It therefore seems unlikely to us that impaired proliferation is the sole reason for the failings in lymphocytes development. The less pronounced increase in proliferation obtained with BrdU could be because of a high level of cell death in the mutant and the resulting loss of some BrdU$^+$ cells. Toy et al. also suggest that a defect in DCK could impair V(D)J recombination (18). In our mutant, we observe a significantly higher level of expression of the CD25/IL-2R α-chain in DN3 cells (Fig. 3C), as observed in cells from mice lacking pre-TCR signaling (27, 28). This could therefore indicate that a defect in dCK might impair TCRβ production or signaling. We were able to measure wt levels of intracellular TCRβ in mutant DN3 cells (Fig. 3D), supporting a normal V(D)J TCRβ recombination in DCK-deficient thymocytes, and therefore pointing toward an impaired TCR signaling in DCK-deficient cells. The phenotypes observed in *memi* mice are comparable with pre-Tα–deficient mice in which development is partially blocked between DN3 and DN4 stages and which present increased proliferation, apoptosis, and memory cells in the periphery (32). Under ADA-deficient conditions, the accumulation of adenosine and deoxyadenosine has been shown to impair TCR signaling and directly induce apoptosis in developing thymocytes, respectively (33–35). Because deoxyadenosine is one of DCK substrate, we could therefore hypothesize that a similar mechanism is operating in *memi* thymus whereby, in the absence of a functional DCK, deoxyadenosine and its derivatives accumulate and affect early thymocytes development through cell-intrinsic impairment of TCR signaling. However, even if severe, this developmental defect is only partial because some cells overcome the DCK deficiency, continue their development, and migrate to the periphery. These cells might, however, represent a limited repertoire of specificity; that is, they are oligoclonal populations expanded by homeostatic proliferation as exemplified with the CD8$^+$ T cell response to LCMV (Fig. 1A). Interestingly, the apparent absence of autoimmunity in this lymphopenic environment might be because of an increase in proportion of regulatory T cells, a hypothesis that deserves further investigation.

In the periphery, two phenomena that have not been described before in a DCK-deficient context are observed: reduced quiescence and increased apoptosis.

Our transfers experiments (Fig. 6) have shown that the proliferation is notably a cell-extrinsic effect of the *memi* mutation as wt cells injected into a $dCK^{mem/mem}$ host undergo proliferation. In a normal peripheral lymphocytic environment, mature T cells remain quiescent for prolonged periods (4). This homeostatic survival relies on contact with self-peptide/MHC complex and IL-7. In an acute lymphopenic environment, these signals will become more available to the remaining naive T cells, resulting in LIP, which restores almost normal levels of T cells in the periphery. In animals chronically lymphopenic because of a complete or severe T cell defect, like TCR$^{-/-}$ or animals with SCID, some transferred T cells will adopt a form of rapid proliferation

FIGURE 5. $dCK^{mem/mem}$ splenocytes are hyperproliferative and apoptotic. (**A**) Mutant CD4$^+$ and CD8$^+$ T cells are significantly hyperproliferative as indicated by BrdU incorporation. The histograms are of two representative mice and the graph representative of three independent experiments; $n \geq 3$. (**B**) Expression of CD44 and CD62L on mutant and wt peripheral blood T cells. These data are representative of three independent experiments; $n \geq 3$. (**C**) Cell-cycle analysis of T lymphocytes using a BrdU/7-aminoactinomycin D staining. The histograms are of two representative mice from three independent experiments. (**D**) Expression pattern

of cell-cycle regulators in $dCK^{mem/mem}$ mice. Western blot analysis was done with samples from spleen (SPL) or inguinal lymph nodes (LN). The experiment was done twice independently with pooled samples of three mice per genotype and per organ. (**E**) Apoptotic CD4$^+$ and CD8$^+$ T cells were detected in the Annexin V$^+$/PI$^-$ quadrant. The histograms are from two representative mice and the graph representative of two independent experiments; $n \geq 4$. *$p < 0.05$, **$p < 0.01$, ***$p < 0.001$.
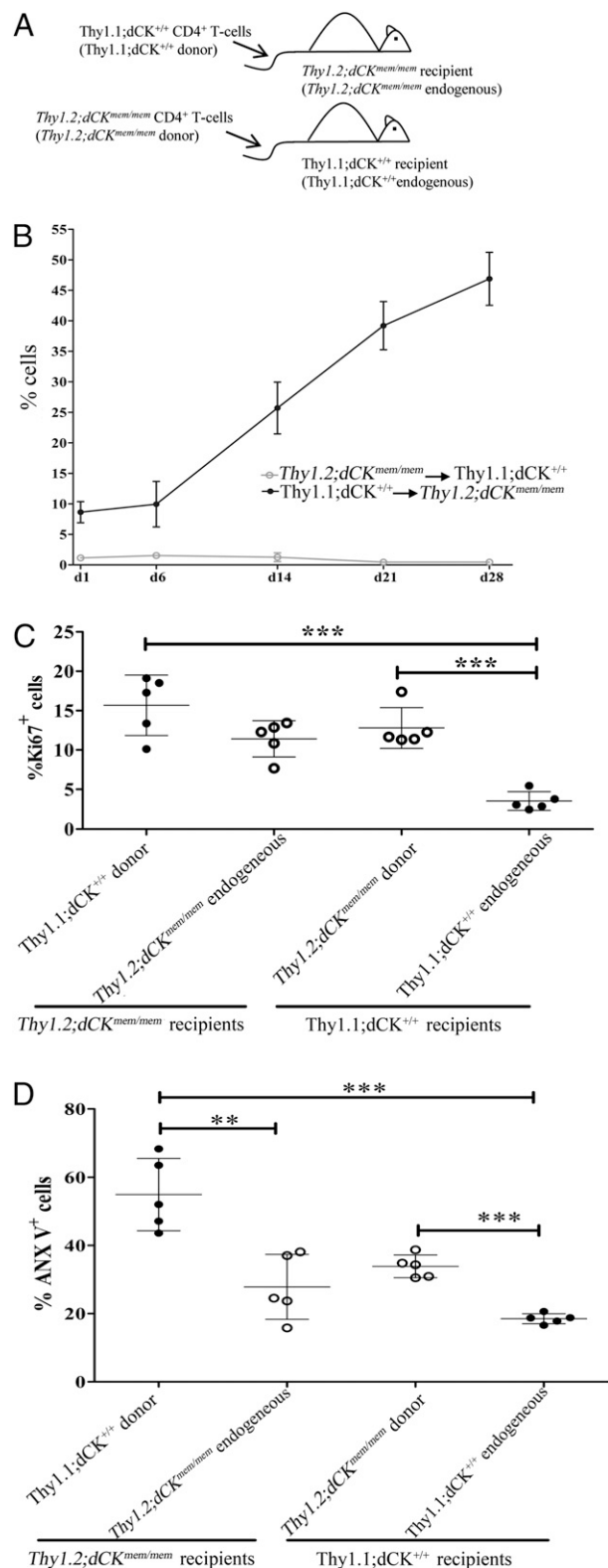
FIGURE 6. Proliferation and apoptosis are controlled by both cell-extrinsic and -intrinsic mechanisms. (**A**) Thy1.1;dCK^{+/+} CD4^{+} T cells were transferred into nonirradiated *Thy1.2;dCK[mem/mem]* recipients and *Thy1.2; dCK[mem/mem]* CD4^{+} T cells into nonirradiated Thy1.1;dCK^{+/+} hosts. All the panels are representative of two independent experiments with five recipients per group. (**B**) The percentage of Thy1.1;dCK^{+/+} donor cells in the *memi* recipient CD4^{+} compartment (black line) and of *Thy1.2;dCK[mem/mem]* donor cells in the wt recipient CD4^{+} compartment (gray line) is represented. (**C**) The proliferation of donor and endogenous cells was measured by Ki67 expression in recipients' splenocytes 35 d after transfer. (**D**)
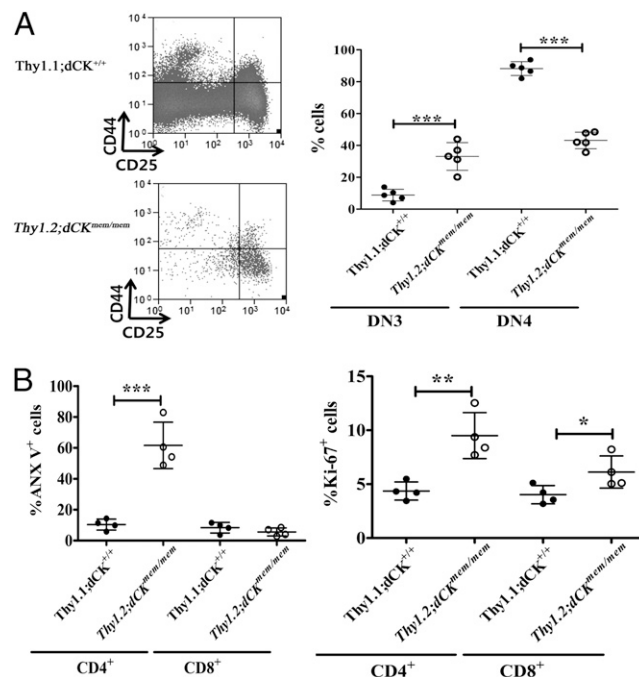
FIGURE 7. *memi* acts on thymocytes' development and peripheral lymphocytes' proliferation and apoptosis in a cell-intrinsic manner. Lethally irradiated wt recipient mice were injected with a 1:1 *Thy1.2; dCK[mem/mem]*:Thy1.1;dCK^{+/+} mixture of BM cells depleted of their mature T cells. The recipient mice were analyzed 5 wk after the injection. (**A**) By gating on either Thy1.1[+] wt or Thy1.2[+] *memi* cells, thymocytes were analyzed in the recipient mice for their DN cell distribution. The histograms are from two representative mice and the graph from two independent experiments; $n \geq 4$. (**B**) Apoptosis and proliferation were analyzed by gating splenic lymphocytes for either Thy1.1[+] wt or Thy1.2[+] *memi* populations and measuring Annexin V or Ki67 expression, respectively. The graphs are representative of two independent experiments; $n \geq 4$. **$p < 0.01$, ***$p < 0.001$.

that is presumably driven by foreign Ags from commensal microflora (4). Finally, a third form of peripheral homeostatic proliferation has been observed when other γ-cytokines are present in excess and in which donor cells undergo a rapid proliferation (36, 37). In our immunodeficient *dCK[mem/mem]* mutants, we observe an important cell proliferation with an effector memory phenotype (CD44^{high}CD62L^{low}). A similar phenotype is found on wt cells transferred into a *memi* environment (Fig. 6C and data not shown), clearly supporting a model of LIP. However, we also found that as late as 35 d after injection in wt hosts, *dCK[mem/mem]* cells still present a memory phenotype (CD44^{high}CD62L^{low}, data not shown), express high levels of Ki67 (Fig. 6C), and are apoptotic (Fig. 6D). If the lymphocyte proliferation and subsequent apoptosis was exclusively driven by the *memi* lymphopenic environment, we would expect that once in a wt immunocompetent host, *dCK[mem/mem]* cells would revert to a more naive quiescent phenotype. This is, however, not the case and the cell-intrinsic effect of *memi* on proliferation and cell death was further supported by the data we obtained with 1:1 chimeric mice (Fig. 7B). The link between an impaired dCK pathway and the continuous inhibition of the Foxo3a pathway that we have observed in *memi* cells deserves further investigation.

Apoptosis of donor and endogenous cells was measured in recipients' splenocytes 35 d after transfer. **$p < 0.01$, ***$p < 0.001$.

The second phenomenon observed is a significant increase in apoptosis. Cells transferred into chronic lymphopenic recipients and undergoing LIP never really manage to reconstitute a normal lymphoid cellularity (38–42). Instead, the donor cells reach a plateau after a few weeks in the host and remain significantly proliferating and susceptible to Bim- and Fas-dependent cell death (30, 31, 41). We therefore propose that the apoptosis observed in wt cells injected into chronically lymphopenic *memi* recipients is a direct consequence of LIP, whereas the increased apoptosis observed in *memi* cells is a cell-intrinsic effect of the mutation and could be a direct consequence of changes in their deoxyribonucleotide triphosphate pools (43–46).

We have presented in this article a new null-mutant allele in the gene coding for DCK, a crucial enzyme of the deoxynucleoside salvage pathway. The phenotypes described make a strong case for a vital, nonredundant, cell-intrinsic role for DCK during lymphocyte development. In addition, our study describes a crucial, nonredundant, and cell-intrinsic role for DCK in peripheral homeostatic proliferation and survival. The data presented in this article support an effect of both the DCK-deficient environment and a cell-intrinsic effect of DCK deficiency on homeostatic proliferation. Our study might also have exposed a potential important regulator of hematopoietic quiescence in human, and our mutant mouse might therefore be a valuable model of hematopoietic proliferative disorder in humans.

Acknowledgments

Disclosures

The authors have no financial conflicts of interest.

References

1. Tzachanis, D., E. M. Lafuente, L. Li, and V. A. Boussiotis. 2004. Intrinsic and extrinsic regulation of T lymphocyte quiescence. *Leuk. Lymphoma* 45: 1959–1967.
2. Brumatti, G., M. Salmanidis, and P. G. Ekert. 2010. Crossing paths: interactions between the cell death machinery and growth factor survival signals. *Cell. Mol. Life Sci.* 67: 1619–1630.
3. Skoda, R. 2007. The genetic basis of myeloproliferative disorders. *Hematology Am. Soc. Hematol. Educ. Program* 2007: 1–10.
4. Surh, C. D., and J. Sprent. 2008. Homeostasis of naive and memory T cells. *Immunity* 29: 848–862.
5. Tothova, Z., and D. G. Gilliland. 2007. FoxO transcription factors and stem cell homeostasis: insights from the hematopoietic system. *Cell Stem Cell* 1: 140–152.
6. Tefferi, A., and D. G. Gilliland. 2007. Oncogenes in myeloproliferative disorders. *Cell Cycle* 6: 550–566.
7. Kaech, S. M., E. J. Wherry, and R. Ahmed. 2002. Effector and memory T-cell differentiation: implications for vaccine development. *Nat. Rev. Immunol.* 2: 251–262.
8. Reichard, P. 1988. Interactions between deoxyribonucleotide and DNA synthesis. *Annu. Rev. Biochem.* 57: 349–374.
9. Eriksson, S., B. Munch-Petersen, K. Johansson, and H. Eklund. 2002. Structure and function of cellular deoxyribonucleoside kinases. *Cell. Mol. Life Sci.* 59: 1327–1346.
10. Nyhan, W. L. 2005. Disorders of purine and pyrimidine metabolism. *Mol. Genet. Metab.* 86: 25–33.
11. Giblett, E. R., A. J. Ammann, D. W. Wara, R. Sandman, and L. K. Diamond. 1975. Nucleoside-phosphorylase deficiency in a child with severely defective T-cell immunity and normal B-cell immunity. *Lancet* 305: 1010–1013.
12. Giblett, E. R., J. E. Anderson, F. Cohen, B. Pollara, and H. J. Meuwissen. 1972. Adenosine-deaminase deficiency in two patients with severely impaired cellular immunity. *Lancet* 300: 1067–1069.
13. Seegmiller, J. E., F. M. Rosenbloom, and W. N. Kelley. 1967. Enzyme defect associated with a sex-linked human neurological disorder and excessive purine synthesis. *Science* 155: 1682–1684.
14. Mandel, H., R. Szargel, V. Labay, O. Elpeleg, A. Saada, A. Shalata, Y. Anbinder, D. Berkowitz, C. Hartman, M. Barak, et al. 2001. The deoxyguanosine kinase gene is mutated in individuals with depleted hepatocerebral mitochondrial DNA. *Nat. Genet.* 29: 337–341.
15. Saada, A., A. Shaag, H. Mandel, Y. Nevo, S. Eriksson, and O. Elpeleg. 2001. Mutant mitochondrial thymidine kinase in mitochondrial DNA depletion myopathy. *Nat. Genet.* 29: 342–344.
16. Zhou, X., N. Solaroli, M. Bjerke, J. B. Stewart, B. Rozell, M. Johansson, and A. Karlsson. 2008. Progressive loss of mitochondrial DNA in thymidine kinase 2-deficient mice. *Hum. Mol. Genet.* 17: 2329–2335.
17. Dobrovolsky, V. N., T. Bucci, R. H. Heflich, J. Desjardins, and F. C. Richardson. 2003. Mice deficient for cytosolic thymidine kinase gene develop fatal kidney disease. *Mol. Genet. Metab.* 78: 1–10.
18. Toy, G., W. R. Austin, H. I. Liao, D. Cheng, A. Singh, D. O. Campbell, T. O. Ishikawa, L. W. Lehmann, N. Satyamurthy, M. E. Phelps, et al. 2010. Requirement for deoxycytidine kinase in T and B lymphocyte development. *Proc. Natl. Acad. Sci. USA* 107: 5551–5556.
19. Arnér, E. S., and S. Eriksson. 1995. Mammalian deoxyribonucleoside kinases. *Pharmacol. Ther.* 67: 155–186.
20. Bergman, A. M., H. M. Pinedo, and G. J. Peters. 2002. Determinants of resistance to 2′,2′-difluorodeoxycytidine (gemcitabine). *Drug Resist. Updat.* 5: 19–33.
21. Lotfi, K., G. Juliusson, and F. Albertioni. 2003. Pharmacological basis for cladribine resistance. *Leuk. Lymphoma* 44: 1705–1712.
22. Du, X., K. Tabeta, K. Hoebe, H. Liu, N. Mann, S. Mudd, K. Crozat, S. Sovath, X. Gong, and B. Beutler. 2004. Velvet, a dominant Egfr mutation that causes wavy hair and defective eyelid development in mice. *Genetics* 166: 331–340.
23. Krol, J., R. E. Francis, A. Albergaria, A. Sunters, A. Polychronis, R. C. Coombes, and E. W. Lam. 2007. The transcription factor FOXO3a is a crucial cellular target of gefitinib (Iressa) in breast cancer cells. *Mol. Cancer Ther.* 6: 3169–3179.
24. Joshi, N. S., W. Cui, A. Chandele, H. K. Lee, D. R. Urso, J. Hagman, L. Gapin, and S. M. Kaech. 2007. Inflammation directs memory precursor and short-lived effector CD8(+) T cell fates via the graded expression of T-bet transcription factor. *Immunity* 27: 281–295.
25. Hoebe, K., Z. Jiang, K. Tabeta, X. Du, P. Georgel, K. Crozat, and B. Beutler. 2006. Genetic analysis of innate immunity. *Adv. Immunol.* 91: 175–226.
26. Jordheim, L. P., E. Cros, M. H. Gouy, C. M. Galmarini, S. Peyrottes, J. Mackey, C. Perigaud, and C. Dumontet. 2004. Characterization of a gemcitabine-resistant murine leukemic cell line: reversion of in vitro resistance by a mononucleotide prodrug. *Clin. Cancer Res.* 10: 5614–5621.
27. Laurent, J., N. Bosco, P. N. Marche, and R. Ceredig. 2004. New insights into the proliferation and differentiation of early mouse thymocytes. *Int. Immunol.* 16: 1069–1080.
28. Mombaerts, P., J. Iacomini, R. S. Johnson, K. Herrup, S. Tonegawa, and V. E. Papaioannou. 1992. RAG-1-deficient mice have no mature B and T lymphocytes. *Cell* 68: 869–877.
29. Murali-Krishna, K., and R. Ahmed. 2000. Cutting edge: naive T cells masquerading as memory cells. *J. Immunol.* 165: 1733–1737.
30. Fortner, K. A., P. Bouillet, A. Strasser, and R. C. Budd. 2010. Apoptosis regulators Fas and Bim synergistically control T-lymphocyte homeostatic proliferation. *Eur. J. Immunol.* 40: 3043–3053.
31. Fortner, K. A., and R. C. Budd. 2005. The death receptor Fas (CD95/APO-1) mediates the deletion of T lymphocytes undergoing homeostatic proliferation. *J. Immunol.* 175: 4374–4382.
32. Bosco, N., F. Agenes, A. G. Rolink, and R. Ceredig. 2006. Peripheral T cell lymphopenia and concomitant enrichment in naturally arising regulatory T cells: the case of the pre-Talpha gene-deleted mouse. *J. Immunol.* 177: 5014–5023.
33. Apasov, S. G., M. R. Blackburn, R. E. Kellems, P. T. Smith, and M. V. Sitkovsky. 2001. Adenosine deaminase deficiency increases thymic apoptosis and causes defective T cell receptor signaling. *J. Clin. Invest.* 108: 131–141.
34. Huang, S., S. Apasov, M. Koshiba, and M. Sitkovsky. 1997. Role of A2a extracellular adenosine receptor-mediated signaling in adenosine-mediated inhibition of T-cell activation and expansion. *Blood* 90: 1600–1610.
35. Lappas, C. M., J. M. Rieger, and J. Linden. 2005. A2A adenosine receptor induction inhibits IFN-gamma production in murine CD4+ T cells. *J. Immunol.* 174: 1073–1080.
36. Cho, J. H., O. Boyman, H. O. Kim, B. Hahm, M. P. Rubinstein, C. Ramsey, D. M. Kim, C. D. Surh, and J. Sprent. 2007. An intense form of homeostatic proliferation of naive CD8+ cells driven by IL-2. *J. Exp. Med.* 204: 1787–1801.
37. Ramsey, C., M. P. Rubinstein, D. M. Kim, J. H. Cho, J. Sprent, and C. D. Surh. 2008. The lymphopenic environment of CD132 (common gamma-chain)-deficient hosts elicits rapid homeostatic proliferation of naive T cells via IL-15. *J. Immunol.* 180: 5320–5326.
38. Murali-Krishna, K., L. L. Lau, S. Sambhara, F. Lemonnier, J. Altman, and R. Ahmed. 1999. Persistence of memory CD8 T cells in MHC class I-deficient mice. *Science* 286: 1377–1381.
39. Cho, B. K., V. P. Rao, Q. Ge, H. N. Eisen, and J. Chen. 2000. Homeostasis-stimulated proliferation drives naive T cells to differentiate directly into memory T cells. *J. Exp. Med.* 192: 549–556.
40. Ge, Q., V. P. Rao, B. K. Cho, H. N. Eisen, and J. Chen. 2001. Dependence of lymphopenia-induced T cell proliferation on the abundance of peptide/MHC epitopes and strength of their interaction with T cell receptors. *Proc. Natl. Acad. Sci. USA* 98: 1728–1733.
41. Goldrath, A. W., L. Y. Bogatzki, and M. J. Bevan. 2000. Naive T cells transiently acquire a memory-like phenotype during homeostasis-driven proliferation. *J. Exp. Med.* 192: 557–564.
42. Tanchot, C., A. Le Campion, B. Martin, S. Léaument, N. Dautigny, and B. Lucas. 2002. Conversion of naive T cells to a memory-like phenotype in lymphopenic hosts is not related to a homeostatic mechanism that fills the peripheral naive T cell pool. *J. Immunol.* 168: 5042–5046.
43. Bradley, M. O., and N. A. Sharkey. 1978. Mutagenicity of thymidine to cultured Chinese hamster cells. *Nature* 274: 607–608.
44. Brox, L., A. Ng, E. Pollock, and A. Belch. 1984. DNA strand breaks induced in human T-lymphocytes by the combination of deoxyadenosine and deoxycoformycin. *Cancer Res.* 44: 934–937.
45. Mathews, C. K., and J. Ji. 1992. DNA precursor asymmetries, replication fidelity, and variable genome evolution. *Bioessays* 14: 295–301.
46. Oliver, F. J., M. K. Collins, and A. López-Rivas. 1996. dNTP pools imbalance as a signal to initiate apoptosis. *Experientia* 52: 995–1000.